Franco Cotana
e-mail: cotana@unipg.it

Federico Rossi
e-mail: frossi@unipg.it

Andrea Nicolini
e-mail: nicolini.unipg@ciriaf.it

Università degli Studi di Perugia, Dipartimento di Ingegneria Industriale, Via G. Duranti 67, 06125 Perugia, Italy

A New Geometry High Performance Small Power MCFC

Molten Carbonate Fuel Cells (MCFC) operate at temperatures ranging from 600 to 700°C; high temperatures allow to obtain low internal losses with large benefits in terms of generated electric power. A new geometry for small sized MCFCs is proposed in this paper. Cell thermofluidodynamic performance has been analyzed through a numerical code. Simulation results verified the suitability of the proposed cell design solutions. A stack consisting of three elementary units has been created in order to experimentally evaluate the proposed cell performance. [DOI: 10.1115/1.1782924]

Introduction

Energy savings and enviromental issues have recently prompted the operators to develop cogenerative energy systems able to simultaneously generate electrical and thermal energies. Fuel Cell Combined Heat and Power systems (FC CHP systems) provide an opportunity of a high-efficient decentralized power supply for the energetic requirements for private and company-sized users. Many companies have developed FC CHP prototypes; however, the short life span of the fuel cells employed, the optimization of operation management and the efficiency of the systems have to be improved. Molten Carbonate Fuel Cells (MCFC) are characterized by high operating temperatures (600–700°C); thus, MCFCs are an optimum solution for FC CHP systems. In particular, high benefits may be achieved in terms of efficiency and chemical reactions kinetics. Economic and technical aspects have actually allowed to develop in particular MCFCs with large power outputs in the range from hundredths of kW to tenths of MW [1]. A small power output MCFC with a novel internal structure is here proposed [2]. A new cylindrical geometry characterizes the proposed cell elements (anode, cathode and matrix). The proposed geometry may allow to obtain benefits with respect to the traditional MCFC in terms of: less construction time and costs thanks to the possibility of using an injection moulding technique; thermal dispersion minimization; global efficiency; minimization of gases tight problems among the cell plates; compression strain uniformity on the contact surface. The proposed cell design solutions have been verified through numerical simulations which have allowed to find inner-cell temperature, pressure and velocity distributions. Simulations and a theoretical investigation have allowed to demonstrate that the proposed solutions are suitable. A measurement campaign is actually in process in order to verify the thermofluidodynamic performances of a stack consisting of three elementary units.

MCFC Traditional Geometry

Conventional MCFCs (developed by main manufacturers until now) are characterized by square or rectangular geometry. While square cells are used for cross-flow MCFC stacks, cells are usually rectangular in co-flow stacks with a shorter length in the gas flow direction and a greater width to reduce the significant axial temperature rise [3]. Cell elements traditional geometry has been here replaced. A cylindrical geometry is proposed which allows to solve the following traditional problems:

- Conventional MCFC elements are traditionally created by the tape casting technique; the proposed cell has a cylindrical geometry. Thus, cell elements may be easily obtained by injection moulding, a moulding technique which may be conveniently used for large scale productions of small size cells, with high advantages in terms of construction times and costs.
- Traditional MCFCs are characterized by high thermal outward dispersions. A cylindrical geometry may allow to minimize thermal dispersions both for the geometry's intrinsic properties and the easiness to insulate a such device. This improves the cell global efficiency.
- Gases tight problems between the cell plates are minimized due in particular to the lack of cell elements corners.
- Compression strain disuniformity on the plate contact surface is reduced due to symmetry of the proposed cell elements.

The Proposed MCFC

Our MCFC module design uses a methane feed, and consists of a catalytic burner, start-up burner and the individual electrochemical cells as shown in Fig. 1. Each individual cell is comprised of cylindrical anode, cathode, matrix and separating plate components. The anode is located at the base of each single cell, and consists of two reaction chambers divided by a separating plate. The upper and lower anodic chambers communicate through a hole in the separating plate center (see Fig. 2). The lower anodic chamber contains ceramic pellets coated with a nickel-based catalyst and is fed by a mixture of methane and steam (see Fig. 1). Here, an endothermic reforming reaction occurs which produces H_2 and CO, subsequently fed to the upper anodic chamber. In the anodic upper chamber, these gases flow over the porous nickel-chrome anode coating; hydrogen reacts with the electrolyte carbonate ion producing H_2O, CO_2 and electrons. Hydrogen is obtained both by methane-steam reaction (reforming, which occurs in the lower anodic chamber) and by CO-steam reaction (shift reaction, which occurs in the upper anodic chamber). Our design allows the efficient production of reforming heat by electrochemical cell reactions. The cathode is placed in the upper portion of the elementary unit (see Fig. 2). Cathodic compartment is fed with a mixture of air and carbon dioxide. In the cathodic chambers, comburent gases flow on the nickel oxide porous cathode; oxygen reacts with CO_2 regenerating the carbonate ion. The matrix is constituted by a lithium aluminate porous element which is soaked in lithium and potassium carbonates (see Fig. 2). The global electrochemical reaction is exothermic. Thus, the elementary cell chemical reactions are

$$CH_4 + H_2O \rightarrow CO + 3H_2 \quad \text{(methane reforming reaction)} \quad (1)$$

$$CO + H_2O \rightarrow CO_2 + H_2 \quad \text{(shift reaction; it occurs in the anodic compartment)} \quad (2)$$

$$H_2 + CO_3^{--} \rightarrow H_2O + CO_2 + 2e^- \quad \text{(anodic reaction)} \quad (3)$$

Manuscript received March 3, 2004; revision received May 4, 2004. Review conducted by: N. M. Sammes.

Copyright © 2004 by ASME

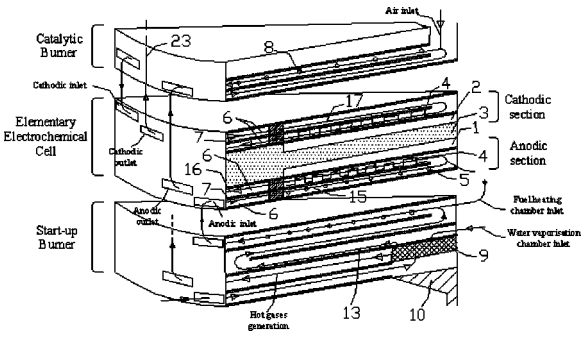

Fig. 1 (a) The proposed MCFC design scheme; (b) distribution and exhaust collectors position

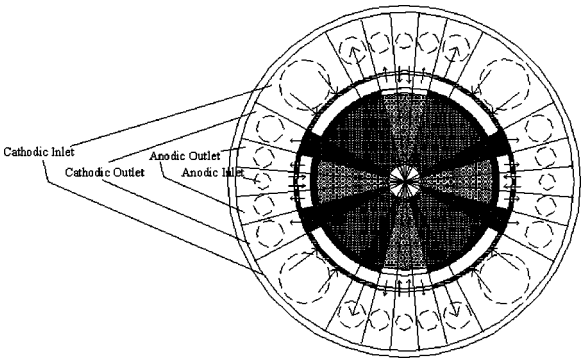

Fig. 3 Inlet and outlet manifolds system for the proposed MCFC

$$CO_2 + 1/2O_2 + 2e^- \rightarrow CO_3^{--} \quad \text{(cathodic reaction)} \qquad (4)$$

The proposed cell is characterized by an internal gas manifold system. In particular, gas inlets and outlets (see Fig. 1) are placed on the stack lateral surface. A double path is designed for each elementary unit both for anodic and cathodic flows: it converges from the external surface to the cell centre at the inlet and it flows in the opposite direction at the outlet. This is obtained by inserting a separating plate for each semi-cell. The flow inversion occurs through a vertical hole placed in the separating plate centre. Electrochemical reactions between gases and electrodes occur at the exit paths. A uniform gases distribution is obtained by creating some holes placed symmetrically on the cell's outside surface. Gases are distributed on a 360 deg angle by making a circular corona shape path on the separating plates zone outside the electrodes. These paths are the cell internal distribution manifolds. Concentric circular ducts are obtained in the separating plates zone inside the electrodes by making decreasing radius annular protrusions (see Fig. 2). Each duct is connected to the adjacent one by means of radial crossings; each protrusion is characterized by the same number of crossings which are placed at the same α angle from one another. Consecutive protrusions openings are staggered by a $\beta = \alpha/2$ angle in order to avoid preferential paths and no-flow zones. A particular manifold system is integrated with the steel coat which externally covers the proposed cell. Steel diaphragms longitudinally divide the space between the steel cylindrical coat and the cell. Diaphragms are combined with the steel coat; ceramic linings are placed on the cell side in order to obtain high performance in terms of gases tight and electrical insulation. Exhaust sections are twice than feeding ones both for anodic and cathodic flows; damages due to gases escapes are minimized by creating each inlet manifold and placing them between two equal outlet manifolds (see Fig. 3). Figure 4 shows an example of the anodic inlet and outlet positions and gases flow paths. Thus, a possible gas escape follows from the feeding manifold to the exhaust one, because gas pressure in the inlet manifold is higher than in the outlet one. A circular base cylindrical shape catalytic burner is placed over the electrochemical stack (see Fig. 1). Catalytic burner allows to: recuperate carbon dioxide produced into the anodic compartments in order to feed the cathodic ones; eliminate fuel residues in the exhaust anodic gases (methane, hydrogen, CO) by catalytic combustion. The catalyser is nickel deposed on a ceramic support. Cathodic reaction is fed by O_2 taken from air which enters in the catalytic burner central zone (see Fig. 1); the following reactions occur:

$$CH_4 + 2O_2 \rightarrow CO_2 + 2H_2O \quad \text{(methane combustion)} \qquad (5)$$

$$CO + 1/2O_2 \rightarrow CO_2 \quad \text{(CO combustion)} \qquad (6)$$

$$H_2 + 1/2O_2 \rightarrow H_2O \quad \text{(hydrogen combustion)} \qquad (7)$$

A modulable power ceramic start-up burner is placed under the stack (see Fig. 1). Start-up burner allows to: generate the hot gases to be led to the cathodic compartment together with the anodic exhaust; fuel heating and water vaporization (see Fig. 1) in order to attain reforming reaction in the anodic compartment. Start-up burner maximum operating conditions occur only at the start-up phase in order to reach the stack nominal temperature and it contributes only to the gases pre-heating when the stack nominal conditions have been achieved.

Theoretical Individuation of the Proposed Cell Performances

Gases flow rates and compositions relative to each elementary cell compartment (internal reformer, anode and cathode) have been theoretically evaluated. Equations (1)–(7) have been used by taking into account chemical reactions evolution and cell configuration. The following assumptions have been made: constant current density on all surfaces of electrodes; fuel is pure methane; the shift reaction completely occurs in the anodic compartment because it is aided by the hydrogen consumption and the steam generation; no conversions occur when methane residues from the reformer contact the anode (very low CH_4 solubility relative to molten carbonates); anodic exhaust fuel residues are completely converted by catalytic combustion; air molar composition at the catalytic burner inlet is O_2 (21 percent), N_2 (79 percent); no reactions occur relatively to N_2; carbon dioxide flow rate at the cathodic inlet has been evaluated by assuming a complete anodic

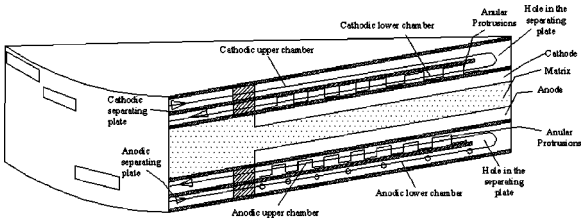

Fig. 2 The proposed MCFC elementary cell

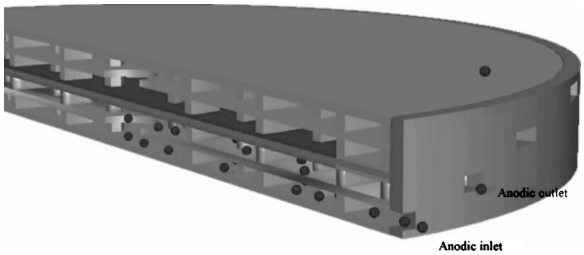

Fig. 4 Inlet and outlet gas flow example relative to the anodic compartment

Table 1 Gases flow rates and composition (30 cm diameter electrodes single cell)

Cell Zone	Molar Flow Rate mol/sec	Molar Composition mol/mol	Mass Flow Rate kg/sec	Mass Composition kg/sec
Reformer inlet	6.993e-4	CH_4:0.333 H_2O:0.667	1.212e-5	CH_4:0.308 H_2O:0.692
Reformer outlet	1.086e-3	CH_4:0.036 H_2O:0.251 H_2:0.534 CO:0.178	1.212e-5	CH_4:0.052 H_2O:0.404H_2:0.096 CO:0.447
Anodic outlet	1.636e-3	CH_4:0.024 H2O:0.438 H_2:0.084 CO:0.053 CO_2:0.401	4.509e-5	CH_4:0.014 H_2O:0.286 H_2:0.006 CO:0.054 CO_2:0.640
Cathodic inlet	4.834e-3	O_2:0.135 CO_2:0.162 H_2O:0.045 N_2:0.658	1.483e-4	O2: 0.141 CO_2: 0.232 H2O: 0.026 N2: 0.601
Cathodic outlet	4.010e-3	O_2:0.095 CO_2:0.058 H_2O:0.054 N_2:0.793	1.154e-4	O_2:0.105 CO_2:0.089 H_2O:0.034 N_2:0.772

exhaust recycle. Constant current density is considered a sustainable hypothesis because the theoretical investigation is carried out in order to evaluate the proposed cell average performances [4]. Cell design parameters values have been determined by means of thermodynamic evaluations on the chemical reactions and MCFC experimental results [4].

Nominal current density design value is 150 mA/cm^2. Reforming is fed by the following methane-steam mixture: CH_4=33 percent; H_2O=67 percent. This composition value was obtained by considering the steam-methane molar ratio able to feed reforming and shift reaction. Besides, this configuration avoids the carbon deposition on the catalyzer for 1 atm pressure and 650°C temperature operative conditions [5]. Equilibrium constant k_{ref} relative to methane steam reforming may be expressed in terms of X average value (converted methane moles) [6]:

$$k_{ref} = \frac{X \cdot (3X)^2 P^2}{(F_{CH_4} - X) \cdot (F_{CH_4} \cdot s/c - X) \cdot [F_{CH_4}(1 + s/c) + 2X]^2} \quad (8)$$

By considering k_{ref}=2.85 atm^2 [6], P=1 atm (a constant indicative value is considered [4]), s/c=2 (steam-methane ratio), F_{CH_4}=1 (methane molar rate at the reformer inlet), Eq. (8) gives X=0.83; this value corresponds to methane utilization degree (U_{CH_4}), if equilibrium conditions are assumed to be obtained in the reformer. A steam-methane ratio equal to 2 (stoichiometric value for the reaction to occur) is considered because ratios of 3–3.5 may allow to obtain best performances but higher steam generation is required. Similarly, by considering anodic electrochemical reaction (see Eq. (3)), shift reaction balance constant k_{sr} may be expressed in terms of Y (CO moles used by shift reaction) [6]:

$$k_{sr} = \frac{[Y + (3X + Y) \cdot U_{H_2}] \cdot [(3X + Y) \cdot (F_{CH_4} - U_{H_2})]}{[X - Y] \cdot [2 - X - Y + (3X + Y) \cdot U_{H_2}]} \quad (9)$$

By considering k_{sr}=2.08 atm^2 [6] and hydrogen utilization factor (H_2 moles which take part in the anodic electrochemical reaction compared to the ones produced by reforming and shift reaction per time unit) U_{H_2}=0.8 (value which is suitable in order to obtain a 150 mA/cm^2 current density value [7,8]), Y is 0.54. Y/X=0.66 represents U_{CO}, CO fraction which is transformed by shift reaction when reaction kinetics allow to obtain equilibrium conditions at the anodic outlet; this condition is hardly obtainable because the composition of gases at the anodic upper chamber varies very quickly due to the simultaneous electrochemical reaction. Thus, U_{CO} (carbon monoxide utilisation factor) was assumed lower (0.55) than the optimum value [9].U_{O_2} (oxygen utilisation factor) determines air flow rate at the cathodic inlet; its value depends on the cathodic reaction stoichiometry and the cell refrigeration requirements. In fact, inlet air flow is usually used as a refrigerant. Thus, U_{O_2}=0.42 was assumed [5]. Gases flow rates, species consumption and generation have been evaluated relatively to a 30 cm diameter electrodes single cell (see Tables 1 and 2).

The first principle of thermodynamics was applied in order to evaluate the heat produced or absorbed by the cell chemical reactions

$$\Delta E = Q + W_{pv} + W_{el} \quad (10)$$

ΔE is the difference between products and reagents internal energies; W_{el}=0 for reforming and shift reaction, because no electric

Table 2 Chemical species consumption and generation

Cell Zone	Reaction	Species	Consumption mol/sec	Consumption kg/sec	Generation mol/sec	Generation kg/sec
Reformer	Steam reforming	CH_4	1.935e-4	3.09e-6		
		H_2O	1.935e-4	3.48e-6		
		H_2			5.804e-4	1.16e-6
		CO			1.935e-4	5.42e-6
Anodic Compartment	Shift reaction	H_2O	1.064e-4	1.92e-6		
		H_2			1.064e-4	2.1e-7
		CO	1.064e-4			
		CO_2		2.98e-6	1.064e-4	4.68e-6
	Anodic Semi-reaction	H_2O			5.494e-4	9.89e-6
		H_2	5.494e-4	1.10e-6		
		CO_2			5.494e-4	2.418e-5
Cathodic Compartment	Cathodic Semi-reaction	CO_2	5.494e-4	2.418e-5		
		O_2	2.747e-4	8.79e-5		

work is produced. Molar reaction heat q was calculated with the following relation:

$$q = \sum_{1}^{Np} n_p h_p - \sum_{1}^{Nr} n_r h_r \tag{11}$$

The following results were achieved:

$$q_{\text{ref}} = [h(\text{CO}) + 3h(\text{H}_2)] - [h(\text{CH}_4) + h(\text{H}_2\text{O})] = 224.8 \text{ kJ/mol } (\text{CH}_4)$$

$$q_{sr} = [h(\text{CO}_2) + h(\text{H}_2)] - [h(\text{CO}) + h(\text{H}_2\text{O})] = -35.5 \text{ kJ/mol (CO)} \tag{12}$$

q_{ref} and q_{sr} values show that methane steam reforming and shift reaction are respectively an endothermic and a slightly exothermic process. Equation (11) may be rewritten for the electrochemical process

$$\Delta h = \sum_{1}^{Np} n_p h_p - \sum_{1}^{Nr} n_r h_r = q_{el} + w_{el} \tag{13}$$

Molar electric work w_{el} was evaluated by electric charge and cell potential V [5]

$$w_{el} = -nFV \tag{14}$$

Cell potential may be evaluated by considering reversible potential ε_{rev}; it represents the maximum potential difference between cell electrodes due to a reversible process. ε_{rev} was evaluated by considering Gibbs energy Δg for an isotherm transformation [6]

$$\Delta g = w_{el} = -nF\varepsilon_{\text{rev}} \tag{15}$$

Cell potential difference may be obtained by ε_{rev} and the current density j [4]

$$V = \varepsilon_{\text{rev}} - j \cdot (R_{\text{ohm}} + Z_a + Z_c) \tag{16}$$

Z_a and Z_c are anodic and cathodic polarization impedances, which may be evaluated by known relations [4]. ε_{rev}, Z_a and Z_c depend on gases partial pressures which vary on the distributor plates due to the chemical reactions evolution. Thus, V is not uniformly distributed on the electrodes surface; electric work was evaluated by assuming a constant V value which is a weighted average value between potentials relative to five circular coronas in which the cell may be divided. V is 0.756 V; the corresponding electric power per cell surface unit is 1130 W/m^2. A 3 kW nominal electric power is obtained by stacking 38 elementary cells. In fact, by substituting V in Eq. (14)

$$q_{el} = -101.71 \text{ kJ/mole}(\text{H}_2) \tag{17}$$

Theoretical DC electric efficiency η_{el} is defined as the ratio between electric power generated by the cell and fuel energy introduced in the reforming section per time unit. Methane molar rate $\text{M.L.}_{\cdot\text{CH}_4}$ at the cell inlet is obtained by Table 1 values. Thus,

$$\eta_{\text{el}} = \frac{\text{V} \cdot \text{j} \cdot \text{S}}{\text{M . L.}_{\cdot\text{CH}_4} \cdot \text{I . C . P.}_{\cdot\text{CH}_4}} = 0.423 \tag{18}$$

Global heat absorbed or generated by the elementary cell were evaluated by multiplying the reaction heat values q_{ref}, q_{sr} eq_{el} respectively with methane, CO and hydrogen molar consumption values: heat absorbed by reforming reaction is 43.5 W/cell; heat generated by shift reaction is 3.8 W/cell; heat generated by electrochemical reaction is 55.9 W/cell. Thus, the cell global heat generation is 16.2 W/cell.

The Proposed Cell Numerical Prediction

The proposed cell thermofluidodynamic performances were evaluated by a finite volume numerical code [10]. The numerical code allowed to evaluate if the proposed gases distribution system configuration was suitable. A simplified numerical model was created because of the highly complex phenomena which characterize the proposed cell: a single elementary cell was analyzed; stationary conditions were considered; gases flows on distribution plates were considered laminar both for cathodic and anodic compartments; external, upper and bottom surfaces were considered adiabatic. Energy, mass, chemical species generation and absorption were simulated by introducing sources and bores in the model. A model of one eighth of the whole cell was simulated due to cell symmetry. The model was meshed in 2,50,6861 tetrahedral elements. The following boundary conditions were assumed: reformer semi-inlet mass flow is 1.515e−6 kg/s (one eighth of the

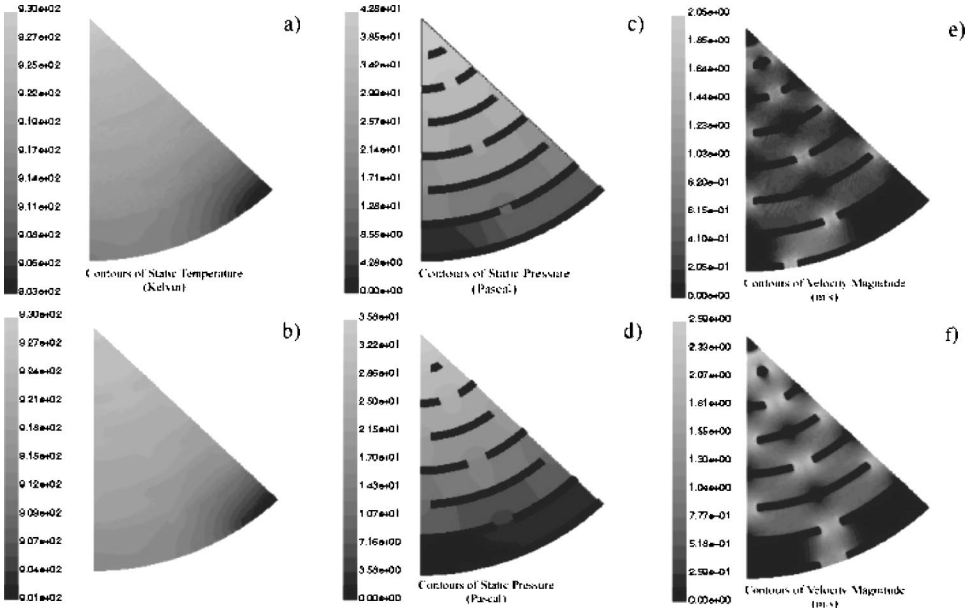

Fig. 5 (a) Anodic upper chamber temperature distribution; (b) cathodic lower chamber temperature distribution; (c) anodic upper chamber pressure distribution; (d) cathodic lower chamber pressure distribution; (e) anodic upper chamber velocity distribution; (f) cathodic lower chamber velocity distribution

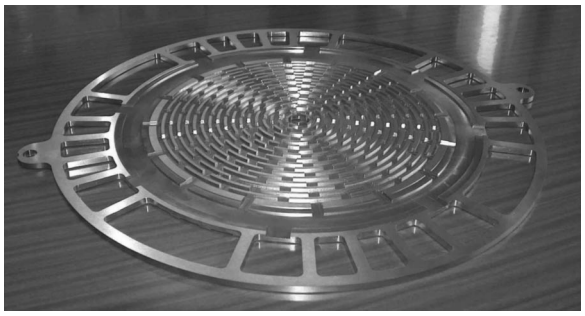

Fig. 6 An element of the MCFC prototype (cathodic lower chamber view)

whole cell); reformer semi-inlet gases composition has been individuated by Table 1 mass fractions; fuel and oxidant inlet temperatures are respectively 873 K and 823 K; cathodic entire inlet mass flow is 1.236e−5 kg/s (1/12 with respect to the whole cell); cathodic semi-inlet mass flow is 6.18e−6 kg/s (1/24 with respect to the whole cell); gases composition assumed for both cathodic inlets are $O_2=0.141$; $CO_2=0.232$; $H_2O=0.026$ (see Table 1); anodic and cathodic exhaust pressure is 1 atm.

For the sake of clarity, Fig. 5 shows simulated temperatures, pressures and velocities distributions relative to anodic upper chamber and cathodic lower chamber. The distribution of gases temperatures is radial and vary in a 30 K range. The highest temperature (930 K) occurs in the cell central zone near the inlet hole; the lowest temperature (about 900 K both for anodic and cathodic gases) occurs in the cell external zone near the exhaust outlets, due to the adjacent feeding gases inlets. The behaviour of gases pressures is radial both for anodic and cathodic compartments. The highest pressure value is in the cell central zone (both for anodic and cathodic compartments). Pressure range is lower in the cathode than in the anode due to the lower gas flow rate. In fact, heat produced by electrochemical reactions is partially absorbed by the internal reformer; thus, oxidant flow for refrigeration is reduced. The behaviour of velocities shows that cathodic and anodic gases flow as designed. Numerical simulations results have shown that the adopted solutions (a new geometry and the innovative gases distribution system) are suitable. Moreover, simulations have verified that

- the temperature differences among the cell zones are minimum (it allows to avoid the degradation phenomena in the hottest zones and to increase cell life)
- thermal integration between reforming and electrochemical sections is efficacious
- cell internal distribution system allows to keep low pressure difference between cathodic and anodic compartment (gases cross-over is avoided [5])

An Experimental Prototype

An experimental prototype was built according to the proposed configuration. It is constituted by a 3 elementary cell stack. Figure 6 shows a stack element (cathodic lower chamber view). An experimental measurement campaign is currently in process in order to verify the cell performances predicted by numerical simulations and theoretical evaluation.

Conclusions

A small power innovative MCFC has been proposed. The cell is characterized by a novel cylindrical shape; gases flow rates and compositions were evaluated relatively to the different cell compartments. The following performances were evaluated: theoretical electric efficiency is 0.427; 3 kW electric power may be obtained by stacking 38 elementary cells. Design solutions are suitable as verified by numerical simulations (in terms of temperatures, pressures and velocities). A cell constituted by three elementary units was created. A thermofluidodynamic measurement campaign is now underway in order to experimentally confirm the simulation results. The proposed cell applications are relative both to civil and industrial users; it may replace traditional gas or double feeding (gas+diesel) boilers as heating plant and simultaneously produce electric energy for the same user. High temperature heat produced by the proposed cell may be used to feed an absorption machine; a circuit dimensions reduction and a thermodynamical cycles energetic efficiencies increase may be obtained. Thus, an energetic and economic estimation of the proposed MCFC for electric and thermal domestic user's requirements will be evaluated.

Nomenclature

F	=	Faraday constant, C/mol
h_p, h_r	=	molar enthalpy relative to the p^{th} product, r^{th} reagent, J/mol
n_p, n_r	=	p^{th} product moles, r^{th} reagent moles, mol
n	=	number of electrons, adimensional
P	=	P pressure, atm
$P_{i,a}$, $P_{i,c}$	=	i^{th} gas partial pressure in the anodic compartment, in the cathodic compartment, atm
$I.C.P._{CH_4}$	=	methane inferior calorific power, J/mol
R_{ohm}	=	impedance due to ohmic polarization, $\Omega \cdot m^2$
S	=	electrode surface m
W_{pv}	=	mechanic work, J

References

[1] Hishinuma, Y., and Kunikata, M., 1997, "Molten Carbonate Fuel Cell Power Generation Systems," Energy Convers. Manage. **38**, (10-13), pp. 1237-1247.

[2] IPASS, 2003, "Dispositivo termoelettrochimico a carbonati fusi per la generazione contemporanea di elettricità e calore a geometria cilindrica," Ministero dell'Industria, del Commercio e dell'Artigianato, Patent N. PG2003A0019, Italy.

[3] Koh, J., and Kang, B. S., 2001, "Theoretical Study of a Molten Carbonate Fuel Cell Stack for Pressurized Operation," Int. J. Energy Res. **25**, pp. 621-641.

[4] Koh, J., Seo, H., Yoo, Y., and Lim, H., 2002, "Consideration of Numerical Simulation Parameters and Heat Transfer Models for a Molten Carbonate Fuel Cell Stack," Chem. Eng. J. **87**(3), pp. 367-379.

[5] Freni, S., Aquino, M., and Passalacqua, E., 1994, "Molten Carbonate Fuel Cell with Indirect Internal Reforming," J. Power Sources **52**(1), pp. 41-47.

[6] Hou, K., and Hughes, R., 2001, "The Kinetics of Methane Steam Reforming Over a Ni/α-Al_2O Catalyst," Chem. Eng. J. **82**(1-3), pp. 311-328.

[7] Miyake, Y., Nakanishi, N., Nakajima, T., Itoh, Y., Saitoh, T., Saiai, A., and Yanaru, H., 1995, "A Study of Heat and Material Balances in an Internal-Reforming Molten Carbonate Fuel Cell," J. Power Sources **56**, pp. 1l-17.

[8] Clarke, S. H., Dicks, A. L., Pointon, K., Smith, T. A., and Swann, A., 1997, "Catalytic Aspects of the Steam Reforming of Hydrocarbons in Internal Reforming Fuel Cells" Catal. Today **38**, pp. 411-423.

[9] Kim, M., Park, H., Chung, G., Lim, H., Nam, S., Lim, T., and Hong, S., 2002, "Effects of Water-Gas Shift Reaction on Simulated Performance of a Molten Carbonate Fuel Cell" J. Power Sources **103**, pp. 245-252.

[10] Fluent 5 User Guide, 1998, Fluent Incorporated.